C113

Luminal ATP concentrations in the renal proximal tubule of the rat following hypotensive haemorrhage

R.M. Vekaria, R.J. Unwin and D.G. Shirley

Physiology, Royal Free & University College Medical School, London, UK

We have demonstrated recently that the luminal concentration of ATP in the S_2 region of the proximal tubule is considerably greater than that in the glomerular filtrate, suggesting ATP secretion into the lumen (Shirley *et al.* 2005a). Other studies have indicated that luminal nucleotides inhibit tubular transport (e.g. Bailey, 2004; Shirley *et al.* 2005b). It has been proposed that ATP release into the lumen might increase under ischaemic conditions, thereby helping to protect the tubular epithelium by inhibiting energy-consuming transport processes (Leipziger, 2003). In the present study we have assessed whether partial renal ischaemia following haemorrhagic hypotension leads to altered intraluminal ATP concentrations.

Male Sprague-Dawley rats were anaesthetised (sodium thiopentone, 100mg kg^{-1}, I.P.) and prepared surgically for micropuncture of the left kidney. During a 1h control period, collections were made from mid-proximal convoluted tubules, each lasting 4 min. All tubular fluid samples were deposited in ice-cold water and frozen, to halt ATP degradation; 6-10 such collections were pooled from each animal. After the control period, eight rats were subjected to an arterial blood loss of 15 ml kg^{-1} body weight; 30 min later, further collections were made from mid-proximal convoluted tubules (experimental period; 1h). Eight rats acted as time controls. All animals were killed humanely at the end of the experiment. ATP concentrations were determined using the luciferin-luciferase enzyme reaction.

Mean arterial blood pressure (MABP) did not change significantly in the time-control animals. In rats subjected to haemorrhage, MABP was 112 ± 4 mmHg (mean ± S.E.M.) during the control period, fell to 42 ± 3 mmHg immediately after bleeding, and recovered partially to 92 ± 2 mmHg during the experimental period (both post-haemorrhage values significantly lower than the control values; $P<0.001$, ANOVA and Student-Newman-Keuls test). In time-control animals, proximal tubular ATP concentrations were 120 ± 15 nmol l^{-1} during the control period and 125 ± 17 nmol l^{-1} during the experimental period (NS, paired *t* test, $P = 0.63$). Corresponding values in bled rats were 120 ± 22 and 153 ± 38 nmol l^{-1} (NS, $P = 0.41$).

Although the possibility of altered ATP metabolism cannot be excluded, these data argue against a major change in proximal tubular secretion of ATP during haemorrhagic hypotension.

Bailey MA (2004). *Am J Physiol Renal Physiol* **287**, F789-F796.

Shirley DG et al. (2005a). *Proceedings of Renal Association, Belfast*, April 2005.

Shirley DG et al. (2005b). *Am J Physiol Renal Physiol* (in press).

Leipziger J (2003). *Am J Physiol Renal Physiol* **284**, F419-F432.

Supported by the National Kidney Research Fund and St Peter's Trust for Kidney, Bladder & Prostate Research.

Where applicable, the experiments described here conform with Physiological Society ethical requirements.

C114

Reconstruction of interpodocyte channels or spaces in the glomerulus show that they inflate when filtration occurs across the glomerular filtration barrier

C.R. Neal, K. Lisowski, H. Kirby, D.O. Bates and S.J. Harper

MVRL, Dept of Physiology, Bristol University, Bristol, UK

Recently, we discovered that the centre of the glomerulus is drained by a series of tributaries between podocytes forming an anastomosing system of channels or interpodocyte spaces (IPS) (Neal, 2003, 2005). The IPS could remove primary urine from the centre of the glomerulus to its periphery and thence into the shell like peripheral urinary space (PUS) which is similar to Bowmans original space of 1842 (Neal, 2005). We have now reconstructed the IPS and studied its dimensions more fully throughout the glomerulus to see how it changes under perfusion compared with non-perfusion conditions.

Kidneys from humanely killed rats were either fixed with glutaraldehyde by immersion (n=3, renal arterial pressure of 0mmHg) or perfusion after a flush of the kidneys with Ringer solution (n=5, renal arterial pressure of 100mmHg throughout). Kidney pieces were postfixed, dehydrated, embedded and serial ultrathin sections of glomeruli were cut. The IPS were reconstructed from electron micrographs of these sections using the Reconstruct program (version 1.0.3.9, John C. Fiala). The general course of the IPS was followed by reconstructing the mean free path of the IPS in the glomerulus. This was complemented by measuring the widths of the IPS. Data were compared using unpaired t tests and Mann-Whitney U tests.

The reconstructions showed that IPS branched by splitting into two and bridging podocytes often temporarily blocked the IPS. The width of the IPS in these selected reconstructions and also in randomly selected central and peripheral locations showed that the IPS was wider in perfusion fixed glomeruli (1.56±0.13μm, n=30, 1-2 glomeruli per rat) and narrower in immersion fixed (non-perfused) glomeruli (0.85±0.05μm, n=25, 1-2 glomeruli per rat; P=0.0001, t test or U test).

While the perfusion pressure (100mmHg) and the absence of balancing colloid from the perfusate suggests that glomerular ultrafiltration should be artificially high, we expect that tubuloglomerular feedback will bring the glomerular filtration rate back to near normal prior to fixation. This suggests that the IPS inflates with fluid under near normal filtration conditions which may be controlled by the constrictions that exist where the IPS meets the PUS (Neal, 2005). The glomerulus inside the Bowmans capsule appears to work in a functionally distended fashion - much like the whole kidney.

Neal CR *et al.*(2003). *J Physiol* **552P**, C26.

Neal CR *et al* (2005). *J Am Soc Nephrol* **16**, 1223-1235.

Supported by The Wellcome Trust (58083) and BHF (BB2000003).

Where applicable, the experiments described here conform with Physiological Society ethical requirements.

C115

Aquaporin 1 is a CO_2 channel in human red cell membranes

G. Gros[1], L.V. Virkki[2], L.S. King[3], W.F. Boron[4] and V. Endeward[1]

[1]Zentrum Physiologie -4220-, Medizinische Hochschule Hannover, Hannover, Germany, [2]Physiologisches Institut, Universitaet Zurich, Zurich, Switzerland, [3]Dept. Medicine, Johns Hopkins University, Baltimore, MD, USA and [4]Dept. Mol. Cell. Physiology, Yale University, New Haven, CT, USA

CO_2 permeability, P_{CO2}, was measured by ^{18}O exchange in human normal and aquaporin 1-deficient (AQP1-deficient (1)) red cells and in Xenopus laevis oocytes expressing human AQP1. In normal red cells we find a P_{CO2} of 0.28 ± 0.21 cm/s (mean ± S.D.; n=70), which is 3-4 orders of magnitude greater than the permeability of this membrane for HCO_3^- (P_{HCO3-}= $1.5x10^{-3}$ cm/s). In the presence of 1 mM of the mercurial pCMBS, P_{CO2} of red cells from normal individuals falls significantly (P<0.05) to 0.07 cm/s (i.e., 25% of normal). In AQP1-deficient red cells from Colton-null individuals, P_{CO2} is also ~25% (P<0.05) of the uninhibited value in red cells from normal individuals. In the AQP1-null cells, pCMBS has no significant effect on P_{CO2}, indicating that the target molecule of pCMBS is indeed AQP1. These results suggest that AQP1 in red cells is the major pathway for molecular CO_2. This view is confirmed by the finding that P_{CO2} of Xenopus laevis oocytes approximately doubles with expression of human AQP1 (P<0.04). In red cells from normal individuals, 100 μM DIDS reduces P_{CO2} from 0.25 cm/s to 0.05 cm/s (P<0.02). In AQP1-null red cells, DIDS reduces P_{CO2} from 0.07 to 0.012 cm/s (P<0.05). This last value may represent the basal P_{CO2} of the membrane due to the lipid phase alone. We conclude that, in contrast to classical views, transport of molecular CO_2 across red-cell membranes occurs mainly via proteins.

Mathai JC, Mori S, Smith BL, Preston GM, Mohandas N, Collins M, van Zijl PC, Zeidel ML & Agre P (1996). J Biol Chem 271, 1309-13.

Supported by the Deutsche Forschungsgemeinschaft, SFB 621.

Where applicable, the experiments described here conform with Physiological Society ethical requirements.

C116

SLC26 anion exchanger activity in the airway epithelial cell line Calu-3

H.E. Moore[1], B. Burghardt[2] and M.C. Steward[1]

[1]Faculty of Life Sciences, University of Manchester, Manchester, UK and [2]MTA-SE Molecular Oral Biology Research Group, Semmelweis University, Budapest, Hungary

The CFTR Cl^- channel activates anion exchangers of the SLC26 family through direct intermolecular interactions (Ko et al. 2004). This may account for the defective HCO_3^- secretion observed in epithelia affected by cystic fibrosis. The Calu-3 cell line, derived from human airway submucosal glands, is a good model for investigating CFTR-dependent HCO_3^- secretion. Our aim was to characterize the apical membrane anion exchanger in these cells and examine the effects of elevated intracellular cAMP on its activity.

Calu-3 cells were grown to confluence on Transwell polyester filters (Corning) and loaded with the pH-sensitive fluoroprobe BCECF. Filters were superfused with HCO_3^--buffered solutions ((mM) 144 Na^+, 5 K^+, 1 Ca^{2+}, 1 Mg^{2+}, 123 Cl^-, 25 HCO_3^-, 1 SO_4^{2-}, 5 Hepes, 10 glucose) and maintained at 37°C on the stage of an inverted fluorescence microscope. Intracellular pH (pH_i) was recorded by standard microfluorometric techniques.

Substitution of Cl^- by gluconate on the basal side of the Calu-3 cells led to an increase in pH_i of 0.28 ± 0.04 (mean ± s.e.m., n = 4, P < 0.01 by paired t test). This was abolished by pre-treatment with 0.1 mM DIDS, consistent with previous reports that the AE2 anion exchanger is expressed at the basolateral membrane (Loffing et al. 2000). In contrast, substitution of Cl^- on the apical side had no effect on pH_i in unstimulated cells, but led to a large and rapid rise of 0.60 ± 0.03 (n = 4, P < 0.001) in cells stimulated with 10 μM forskolin. This alkalinization was unaffected by DIDS even at 1 mM. The recovery of pH_i following restoration of apical Cl^- could be mimicked by I^- and formate but not by SO_4^{2-} or oxalate.

RT-PCR performed on RNA extracted from Calu-3 cells revealed transcripts for several members of the SLC26 family. These included pendrin (SLC26A4) which, unlike most other members of the family, is unable to transport divalent anions and is relatively insensitive to DIDS (Mount & Romero, 2004). We therefore propose that pendrin may be the apical anion exchanger in Calu-3 cells and that its activity is markedly stimulated by cAMP, most probably through interaction with CFTR.

Ko SBH *et al.* (2004). *Nature Cell Biol* **6**, 343-350.

Loffing J *et al.* (2000). *Am J Physiol* **279**, C1016-C1023.

Mount, DB & Romero MF (2004). *Pflugers Arch* **447**, 710-721.

Supported by the Wellcome Trust, Royal Society and Hungarian Academy of Sciences.

Where applicable, the experiments described here conform with Physiological Society ethical requirements.

C117

Acute effects of cortisol on the activity of Na^+-H^+ exchanger (NHE) in the human placental syncytiotrophoblast: receptor mediation and gender effect

P.F. Speake, S.L. Greenwood, J.D. Glazier and C.P. Sibley

Division of Human Development, University of Manchester, Manchester, UK

NHE activity in human placental syncytiotrophoblast is stimulated acutely by cortisol (CORT) in the presence of the 11-β-hydroxysteroid dehydrogenase type 2 (11-β-HSD-2) inhibitor, carbenoxolone (CBNX, Speake *et al.* 2004a). In this study we investigated the involvement of glucocorticoid (GR) and mineralocorticoid (MR) receptors in this response and whether there is a gender effect.

Villous fragments from term human placenta (obtained as approved by Local Research Ethics Committee) were incubated in Tyrode solution (containing in mM; NaCl 135, KCl 5, $CaCl_2$ 1.8, $MgCl_2$ 1, Mops 10 and glucose 5, pH 7.4) with 1μM of the intracellular pH (pH_i) sensitive dye, BCECF-AM (Molecular Probes), for 5min at 37°C, washed in Tyrode solution without

BCECF and incubated at 37°C for 5min. BCECF fluorescence and NHE activity were measured as described previously (Speake *et al.* 2004b) and expressed as pH units/s (mean±S.E.M., n=number of placentas). CBNX (100μM) and/or CORT (1μM,) were added for 3min, in the absence of Na^+ following the 5min, 20mM NH_4Cl pulse and in Na^+ Tyrode solution during the recovery period. Spironolactone (1μM), an inhibitor of MR, and mefiprestone (1μM), an inhibitor of GR were added to the incubation medium during the NH_4Cl pulse and were present in all subsequent solution changes.

There was no difference in the resting pH_i between male and female syncytiotrophoblast (7.34±0.03, n=7 compared to 7.36±0.05, n=10, respectively). The control rate of recovery from an acid load was 0.0050±0.0007pH units/s (n=17) and there was no difference between male or female placentas. Combined application of CBNX and CORT significantly ($p<0.05$ unpaired Student's| t test) increased the rate of recovery in female (0.0089±0.0015pH units/s, n=10) compared to male (0.0060±0.0012pH units/s, n=7) placentas. In female placentas the increase in recovery with the combined incubation of CBNX and CORT was significantly reduced to levels no different from controls by mefiprestone (0.0042±0.0009pH units/s, n=10 $p<0.05$ repeated measured ANOVA followed by Dunns' post hoc test) and unaffected by spironolactone (0.0067±0.0012pH units/s, n=10).

In conclusion the activity of syncytiotrophoblast NHE's is increased by acutely elevated CORT levels only in the presence of CBNX in female placentas only and this increase is mediated through GR. The gender dependent effect may be due to differences in 11-β-HSD-2 expression or activity (Murphy *et al.* 2003) and/or differential GR expression between male and female placentas (Clifton & Murphy, 2004).

Clifton VL & Murphy VE (2004). Placenta 25, S45-52.

Murphy VE et al. (2003). Am J Respir Crit Care Med 168, 1317-1323.

Speake PF et al. (2004a). Placenta 25, A19.

Speake PF et al. (2004b). J Physiol 555.P, C106.

Supported by The Wellcome Trust.

Where applicable, the experiments described here conform with Physiological Society ethical requirements.

C118

Insulin restores D-glucose inhibition of adenosine transport through activation of equilibrative nucleoside transporter 2 in human umbilical vein endothelium

G. Munoz[1], R. San Martin[1], M. Gonzalez[1], M. Pastor-Anglada[2], P. Casanello[1] and L. Sobrevia[1]

[1]Cellular and Molecular Physiology Laboratory (CMPL), Department of Obstetrics and Gynaecology, Medical Research Centre (CIM), School of Medicine, Pontificia Universidad Catolica de Chile, Santiago, Chile and [2]Departament de Bioquimica i Biologia Molecular, Universitat de Barcelona, Barcelona, Spain

Insulin and hyperglycaemia induced vasodilatation is explained by activation of endothelial L-arginine transport and nitric oxide (NO) synthesis (L-arginine/NO pathway)(Gonzalez *et al.* 2004). Hyperglycaemia reduces uptake of the endogenous nucleoside adenosine in human umbilical vein endothelium (HUVEC). Since biological effects of adenosine depend on an efficient uptake via human equilibrative nucleoside transporters 1 (hENT1) and hENT2 in HUVEC (Vasquez *et al.* 2004), changes in hENT1 and/or hENT2 expression and activity are crucial to keep physiological levels of extracellular adenosine. We studied whether insulin alters adenosine transporters in HUVEC.

Cells were cultured in medium 199 containing 20% bovine serum, 3.2 mM L-glutamine, 100 iu/ml penicillin-streptomycin (37°C, 5% CO_2). Passage 2 cells were exposed (0-24 h) to medium containing 5 (normal) or 25 mM (high) D-glucose and insulin (0.001-100 nM). Adenosine transport ([^{3}H]adenosine, 5-500 μM, 4 μCi/ml, 37°C, 20 s) was measured in absence or presence of nitrobenzylthioinosine (NBMPR, 0.001-100 μM) or hypoxanthine (2 mM). Specific [^{3}H]NBMPR equilibrium binding (0.01-5 nM, 30 min) was measured. hENT1 and hENT2 mRNA were quantified by real-time PCR and proteins were detected by Western blot. Overall adenosine transport (hENT1- and hENT2-mediated) was significantly ($P<0.05$, unpaired Student's *t* test, values are means ± S.E.M., n=4-12) increased (2.1-fold) by insulin, associated with increased V_{max} for hENT2-, but reduced V_{max} for hENT1-mediated transport in normal D-glucose. Insulin also increased hENT2 (1.7-fold), but reduced (45±12%) hENT1 protein abundance and mRNA number of copies (66±10%), and returned high D-glucose induced reduction of hENT1 and hENT2 mRNA expression, and hENT2 protein abundance to values in cells in normal D-glucose. However, insulin did not alter ($P>0.05$) hENT1 protein abundance. Insulin and high D-glucose increased eNOS expression (protein and mRNA) and activity (1.2±0.2, 3.1±0.4 and 2.6±0.1 pmol/μg protein/30 min for control, insulin and high D-glucose, respectively). Insulin effect on hENT1 was blocked by N^G-nitro-L-arginine methyl ester (L-NAME, eNOS inhibitor), and only hENT1-mediated transport was reduced by *S*-nitroso-N-acetylpenicillamine (SNAP, NO donor). Thus, insulin increases overall adenosine transport by increasing hENT2 expression and activity, a phenomenon that does not involve NO. However, NO synthesis is required for insulin-inhibition of hENT1 transport, but not for its expression.

Gonzalez M *et al.* (2004). *Pflugers Arch-Eur J Physiol* **448**, 383-394.

Vasquez G *et al.* (2004). *J Physiol* **560**, 111-122.

FONDECYT 1030781 & 1030607 (Chile). M.G. holds a CONICYT-PhD fellowship.

Where applicable, the experiments described here conform with Physiological Society ethical requirements.

PC165

Use of pCEP4 vector for simple and rapid establishment of stable cell-lines and long-term gene expression

R. Flynn[1], D. O'Sullivan[2], A.M. Sullivan[2] and P.T. Harrison[1]

[1]Physiology, University College Cork, Cork, Ireland and [2]Anatomy, University College Cork, Cork, Ireland

For many studies, transient transfections are of limited use due to a low percentage of cells transfected and short-term duration of gene expression, whereas construction of stable cell-lines can be labour-intensive and take many months. We report the use of an episomal replicating vector and characterise its use in the simple and rapid production of stable cell lines using a fluorescent reporter protein in two cell lines.

The cDNA for a variant of enhanced yellow fluoresecent protein (EYFP; Jayaraman et al. 2000) was sub-cloned into the *Sal*I restriction sites of pCEP4 (Invitrogen Ltd). CFTE cells (Gruenert et al. 2004) were seeded at a density of 200,000 per 35 mm dish 24 h prior to transfection. 2μg DNA was mixed with 6μl Lipofectamine (Invitrogen Ltd) in 3 ml serum-free culture medium, incubated at room temperature for 15 min and added to cells. Medium was replaced after 5 h with fresh medium supplemented with 10% foetal calf serum. 24 h post-transfection, cells were observed by fluorescence microscopy and approximately 10% of cells were expressing EYFP. Cells were treated with hygromycin to kill non-transfected cells. Over a 21 day period, the percentage of cells expressing EYFP increased such that essentially all cells were expressing EYFP. When hygromycin was removed, essentially all cells remained yellow for a further 3 weeks, although a slight decrease in intensity was observed.

SHSY-5Y cells (Vinores et al. 1984) were cultured and transfected in a similar manner. 24 h post-transfection approximately 10% of cells were judged to be expressing the variant EYFP. Over a 21 day period, in the absence of hygromycin, the percentage of cells expressing variant EYFP remained constant. Towards the end of this period, a few colonies comprising a small number (less than 10) of yellow cells began to emerge within the population. All cells in each colony had the same level of fluoresence, but the level of fluorescence differed between colonies. Such an observation is consistent with the integration of the pCEP4-EYFP plasmid into different regions of the genome resulting in different levels of gene expression. Colonies such as this would be expected to give rise to conventional stable cell lines. However, to ensure a homogeneous stable population, they would first need to be cloned, and then amplified. This would take at least another 3 weeks to reach 10^6 cells.

In summary, the use of episomally replicating plasmids, such as pCEP4, can be used to generate stably expressing cells in the absence of hygromycin selection, or select stable cell-lines within 3 weeks in the presence of hygromycin selection, with minimal manipulations. When hygromycin selection is withdrawn, gene expression remains stable for at least 3 weeks.

Jayaraman S *et al.* (2000). *J Biol Chem.* **275**, 6047-50.

Gruenert DC *et al.* (2004). *J Cyst Fibros.* **2**, Suppl 2:191-6.

Vinores SA *et al.* (1984). *Cancer Res.* **44**, 2595-9.

This work was supported by HEA/PRTLI3 and Health Research Board.

Where applicable, the experiments described here conform with Physiological Society ethical requirements.

PC166

Cytokines, hepatic hepcidin production and iron transport by intestinal epithelial cells

M. Mascarenhas[1], D. Johnson[2], P. Sharp[3] and S. Srai[1]

[1]Biochemistry and Molecular Biology, Royal Free and University College Medical School, London, UK, [2]School of Biomedical and Molecular Sciences, University of Surrey, Guildford, UK and [3]School of Health & Life Sciences, Kings College London, London, UK

Hepcidin is widely perceived to act as the master physiological regulator of body iron metabolism (reviewed in Ganz, 2005). Interestingly, a number of studies have shown that hepcidin levels are inappropriately high in inflammatory conditions and this can lead to the development of the anaemia of chronic disease. Elevated production of hepcidin in these pathological situations is thought to be regulated by pro-inflammatory cytokines, in particular IL-6. Our work and that of others suggests that the gut is a target organ for the action of cytokines (Johnson et al. 2004). Therefore, our current study has investigated the link between cytokines, hepcidin production and the effects on intestinal iron transporter expression.

Studies were performed on established hepatic (HuH7) and intestinal (Caco-2) cell models. Prior to experimentation, cells were stimulated with either TNFα or IL-6 (10ng/ml). HuH7 cells were then assessed for hepcidin mRNA levels by quantitative PCR. Caco-2 cells were used to measure changes in the expression of the divalent metal transporter (DMT1) and iron regulated transporter (IREG1) protein by Western blotting. In additional experiments, Caco-2 cells were exposed to conditioned medium produced from IL-6 stimulated HuH7 cells. Data are mean ± S.E.M. from 3-6 experiments in each group. Statistical analysis was performed using Student's unpaired t test and differences were considered significant when $P<0.05$.

Hepcidin levels were significantly increased in HuH7 cells stimulated with IL-6 (415 ± 15%, $p<0.002$) but not in those exposed to TNFα (110 ± 18%) compared with the unstimulated controls. In Caco-2 cells, TNFα induced a decrease in DMT1 protein levels (-32.1 ± 4.5%, $p<0.005$) compared with the controls, whereas there was no effect of IL-6 (-5.7 ± 8.0%). IREG1 levels were not altered in Caco-2 cells by either cytokine. Interestingly, exposure of Caco-2 cells to conditioned medium produced from IL-6 stimulated HuH7 cells resulted in a significant decrease in DMT1 protein expression (-33.1 ± 4.9%, $p<0.01$). Incubation with synthetic hepcidin also decreased Caco-2 cell DMT1 levels (Yamaji et al. 2004). Taken together with our current data, this suggests that hepcidin may be the active agent in the conditioned medium. Importantly for intestinal iron absorption, our data suggest that the response to the cocktail of cytokines released in inflammatory conditions is not uniform. We propose that at least two distinct pathways exist that converge on intestinal enterocytes to regulate the rate of iron absorption. In this model, some cytokines (such as TNFα) have a direct effect on the intestinal mucosa to regulate dietary iron assimilation, whereas others (e.g. IL-6) act indirectly first stimulating the release of hepcidin which then elicits its inhibitory action on intestinal iron transport.

Ganz T (2005). Best Pract Res Clin Haematol 18, 171-182.

Johnson et al. (2004). FEBS Lett 573, 195-201.

Yamaji et al. (2004). Blood 104, 2178-2180.

This work was funded by BBSRC and MRC.

Where applicable, the experiments described here conform with Physiological Society ethical requirements.

PC167

Lateral diffusion of CFTR on the cell surface measured using an engineered biotinylation target sequence

I.R. Bates[1], Y. Luo[1], J. Liao[1], A. Bachir[2], D.L. Kolin[2], B. Hebert[3], P.W. Wiseman[4] and J.W. Hanrahan[1]

[1]Physiology, McGill University, Montreal, QC, Canada, [2]Chemistry, McGill University, Montreal, QC, Canada, [3]Physics, McGill University, Montreal, QC, Canada and [4]Chemistry and Physics, McGill University, Montreal, QC, Canada

Lateral mobility of the cystic fibrosis transmembrane conductance regulator (CFTR) chloride channel and its potential interactions with other proteins were studied by engineering a biotinylation target sequence into an extracellular loop and stably expressing the tagged construct in baby hamster kidney (BHK) cells. The target sequence was specifically biotinylated on intact cells by adding recombinant biotin ligase to the bath solution. Inserting the sequence had little effect on CFTR protein expression according to Western blots, and robust channel activation by cAMP was demonstrated by iodide efflux and patch clamp assays. Confocal microscopy of cells exposed to fluorophore-conjugated streptavidin revealed strong plasma membrane staining of cells expressing biotinylatable wild-type CFTR, but not cells expressing a tagged version of the disease-associated mutant ΔF508. Lateral mobility of CFTR was studied by measuring fluorescence recovery after photobleaching (FRAP) and by image correlation spectroscopy (ICS). FRAP recovery curves were consistent with a randomly diffusing population of CFTR channels with an immobile population of ~20%, and yielded an effective diffusion coefficient $D = 1.4 \pm 0.6 \times 10^{-10}$ cm^2 s^{-1} based on simulated diffusive recovery into a strip bleach. By contrast, ICS under the same conditions indicated a diffusion coefficient of $3.8 \pm 1.7 \times 10^{-11}$ cm^2 s^{-1} (mean ± S.E.M., n = 20 cells); i.e. approximately four-fold slower. Computer simulations revealed that FRAP would generate faster diffusion coefficients than ICS when there is a confined, slowly moving population. To investigate possible protein-protein interactions that might account for the immobile pool, tagged CFTR was co-expressed with clathrin-GFP or glycosylphosphoinositol (GPI)-GFP, and visualized by confocal microscopy after biotinylation and binding of fluorophore-conjugated streptavidin. CFTR on the cell surface was partially co-localized with clathrin-GFP but not with GPI-GFP, suggesting that clathrin coated pits, but not lipid rafts, may contribute to the immobile population of CFTR channels.

This work was supported by grants from the Canadian Institutes of Health Research, Canadian CF Foundation, CF Foundation (U.S.A.) and National Institutes of Health (NIDDK) to J.W.H., and the Natural Sciences and Engineering Research Council (Canada) to P.W.W.

Where applicable, the experiments described here conform with Physiological Society ethical requirements.

PC168

Taste chemoreception in the blowfly is affected by octopamine and serotonin by way of modulation of the transepithelial potential (TEP)

G. Sollai, R. Crnjar, A. Liscia, C. Masala, P. Angioni and P. Solari

Experimental Biology, University of Cagliari, Cagliari, Italy

Octopamine (OA) and serotonin (SR) are multifunctional biogenic amines that act as neuromodulators or neurotrasmitters of many physiological processes in invertebrates, including central as well as peripheral nervous functions. Several studies suggest that both OA and SR are involved in chemoreception mechanisms, possibly by modulating the transepithelial potential (TEP), for which a major role has been proposed in the generation of the receptor potential [1, 2, 3], sustained by an electrogenic potassium transport from sensillar accessory cells. Nevertheless, the effects of OA and SR, particularly on gustatory systems, are little understood. Thus, by means of electrophysiological techniques, we investigated whether octopamine and serotonin affect the TEP in the labellar taste chemosensilla of the blowfly Protophormia terraenovae. Drugs were dissolved in saline at 0.1 and 0.5 mM and injected (approx. 1 µl) near the base of the labellum using a fine tipped glass capillary connected to a pressure micro-injector, with the aim of reaching, via hemolymph, the accessory cells where the putative K^+-dependent TEP generation mechanisms are located [4]. TEP values were monitored before (controls) and for 20 min after drug injection. Statistical differences were evaluated by means of the Student's t test with a 95% confidence level.

Figure 1 shows that application of OA significantly decreases the TEP in a dose-dependent manner, from 42.11 ± 1.61 to 28.03 ± 1.77 mV at the lower tested concentration (0.1 mM) and from 46.17 ± 4.04 to 18.17 ± 2.88 mV at the higher (0.5 mM). Similarly, 0.1 mM SR reduces the TEP value from 42.17 ± 2.20 to 25.23 ± 2.18 mV, while at the highest concentration the TEP is nearly abolished (44.06 ± 2.48 to 5.00 ± 1.65 mV; Fig. 2). Injection of saline does not significantly alter the TEP values.

In conclusion, both OA and SR appear to modulate the TEP amplitude, possibly by affecting the electrogenic potassium transport, according to the generally accepted hypothesis that a vacuolar-type H^+-ATPase and the subsequent K^+/H^+ antiport are involved in the mantainance of the TEP, as described in other insect epithelia, such as Malpighian tubules in Drosophila melanogaster [5] or olfactory sensilla in the sphinx moth [2].

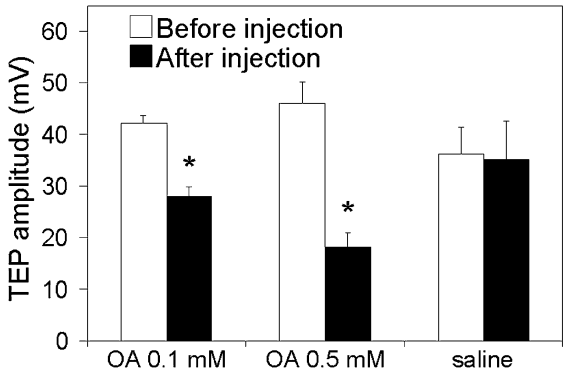

Figure 1. Mean values ± S.E.M. (vertical bars) of TEP amplitudes (mV) recorded before and 20 min after injection of 0.1 or 0.5 mM octopamine (OA) and saline. Number of sensilla tested: 52-96. *Significant difference (p≤0.05) between TEP values before and after injection.

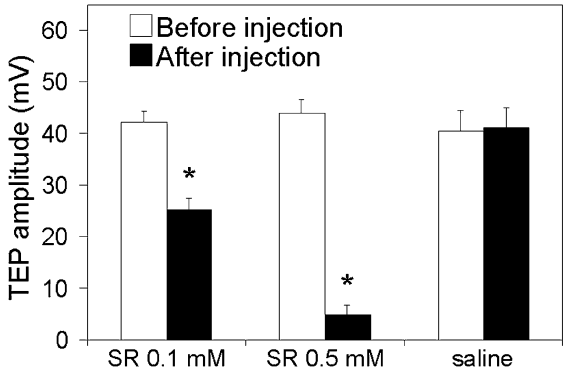

Figure 2. Mean values ± S.E.M. (vertical bars) of TEP amplitudes (mV) recorded before and 20 min after injection of 0.1 or 0.5 mM serotonin (SR) and saline. Number of sensilla tested: 52-96. *Significant difference (p≤0.05) between TEP values before and after injection.

Thurm U & Wessel G (1979). J Comp Physiol 134, 119-130.

Dolzer J et al. (2001). J Exp Biol 204, 2781-2794.

Pophof B (2000). J Comp Physiol 186, 307-313.

Wieczorek H (1982). J Comp Physiol 148, 303-311.

Linton SM & O'Donnell MJ (1999). J Exp Biol 202, 1561-1570.

This work was partly supported by the MIUR.

Where applicable, the experiments described here conform with Physiological Society ethical requirements.

PC169

The effect of M1 and M3 muscarinic receptor antagonists on acetylcholine-induced liquid and mucus secretion from intact porcine bronchi

E. Husband and S. Inglis

Maternal and Child Health Sciences, University of Dundee, Dundee, UK

Acetylcholine (ACh) stimulates an increase in potential difference (PD) across intact porcine bronchi due to stimulation of Cl^- and HCO_3^- secretion (Inglis *et al* 1996). This PD response has

been shown to be mediated largely by the M3 muscarinic receptor subtype (Husband & Inglis, 2004) which is expressed along with the M1 subtype in airway submucosal glands (Mak & Barnes, 1990). The aim of this investigation was to study the liquid and mucus secretions produced in porcine bronchi in response to ACh stimulation and investigate the effect of M1 or M3 antagonism on the volume and composition of these secretions.

The protocol used was similar to that described previously (Ballard *et al.* 1999). Cotswold pigs (~15kg) were anaesthetised with inhaled halothane and killed by intravenous overdose of sodium pentobarbitone. The lungs were removed and the bronchi dissected free. Side branches were ligated and the bronchi warmed to 37°C in a tissue bath. The lumen of each bronchus was cleared of liquid and mucus and the tissue was mounted onto a tubular glass support suspended in a beaker of HCO_3^- buffered solution (gassing with 95% O_2-5% CO_2 to maintain pH 7.4) into which the relevant antagonists were added. Antagonists against M1 and M3 subtypes used in these experiments were pirenzipine (PZ) and 4-diphenylacetoxy-N-methylpiperidine methiodide (4-DAMP), respectively. At the end of each experiment all accumulated liquid and mucus was aspirated from within the lumen and transferred to an eppendorf tube. The collected solutions were weighed and dried to distinguish between liquid and solid (mucus) components.

Both antagonists significantly reduced the total volume secreted in response to stimulation with 50μM ACh in a concentration dependent manner (Student's paired t test, $P<0.05$). 4-DAMP was found to be 106 times more potent than PZ as an inhibitor of liquid secretion with IC_{50} values of 16.00 ± 1.00 nM (n = 25; means ± S.E.M.) and 17.00 ± 1.86 μM (n = 38), respectively. This suggests the M3 subtype is responsible for mediating liquid secretion from the submucosal glands since PZ is relatively non-specific for the M1 receptor at these concentrations. 4-DAMP pre-treatment also significantly reduced the solid component of secretion (IC_{50} = 13.00 ± 1.02 nM, n = 25) while the response to PZ could not be plotted sigmoidally. This suggests the M3 subtype is responsible for mediating mucus secretion with M1 playing a minor role if any. In conclusion, ACh-evoked stimulation of liquid and mucus secretion in porcine bronchi is mediated primarily by the M3 receptor.

Ballard ST *et al.* (1999). *Am J Physiol* **277**, L694-L699.

Husband EM & Inglis SK (2004). *J Physiol* **557P**, PC39.

Inglis SK *et al.* (1996). *Am J Physiol* **270**, L289-L297.

Mak JCW & Barnes PJ (1990). *Am Rev Respir Dis* **141**, 1559-1568.

Where applicable, the experiments described here conform with Physiological Society ethical requirements.

PC170

Regulation of Na^+ transport in airway epithelia by intracellular pH (pH_{in})

M. Constable and S. Inglis

Maternal and Child Health Sciences, University of Dundee, Dundee, UK

Changes in pH_{in} have long been known to alter the rate of Na^+ transport across Na^+-transporting tight epithelia (1, 3). The aim of this current study was to investigate the effect of changes in pH_{in} on Na^+ absorption across H441 cells, a Na^+ absorbing human airway epithelial cell line. Cells were grown to confluence on Snapwell filters (Costar) and mounted in Ussing chambers (1cm^2 exposed surface area, chamber volume 1-1.5ml). The apical and basolateral chambers were then continuously perfused with HCO_3^- -buffered Krebs solution (37°C, ~1ml min^{-1}). Cells were maintained under open circuit conditions until transepithelial potential difference (PD) had stabilised (15-30min). Mean PD, short circuit current (Isc) and transepithelial resistance (Rt) under those conditions were 16.6±2.8mV, 54.5±6.0μAcm^{-2} and 292±22Ωcm^2 respectively (n=6). Transepithelial PD was then clamped at 0mV using a voltage clamp and the current required to maintain this PD (Isc) was continually monitored and recorded to computer disk. Ammonium chloride (25mM) was added to both sides of the epithelium to alkalinise pH_{in} and this induced an initial rise in Isc (i-ii in Figure). Isc then began to fall, presumably as pH_{in} began to acidify (ii-iii), before subsequent removal of NH_4Cl, which acidifies the cells, induced a large inhibition of Isc (iii-iv). Isc then slowly recovered (iv-v), presumably as the cellular pH_{in} regulatory mechanisms returned pH_{in} to normal levels. Addition of apical amiloride (10μM) inhibited this effect of changing pH_{in} on Isc, suggesting that the effects are mediated by a change in Na^+ transport. Addition of 5-(N-Ethyl-N-isopropyl) amiloride (EIPA; 100μM), a Na^+/H^+ exchange inhibitor, had no effect on either the initial rise in Isc or the subsequent fall but did block the recovery of Isc towards the basal level (iv-v). Presumably it inhibited the recovery of pH_{in} from acidosis and thus the Isc remained depressed. In summary, alkalinisation stimulates Na^+ absorption across H441 airway epithelial cells, whilst acidification inhibits Na^+ transport. These results show that in common with Na^+ transport across tight epithelia (1-3) Na^+ absorption in airway epithelia is acutely dependent on pH_{in}.

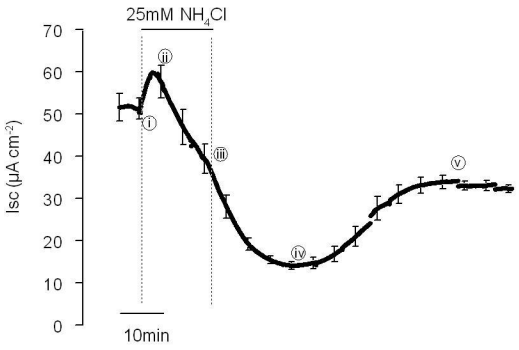

Figure shows mean sem (n=5) Isc across monolayers of H441 cells mounted in a perfused Ussing chamber.

Harvey, B. J., S. R. Thomas, and J. Ehrenfeld. Intracellular pH controls cell membrane Na+ and K+ conductances and transport in frog skin epithelium. Journal of General Physiology 92: 767-791, 1988.

Palmer, L. G., and G. Frindt. Effects of cell Ca and pH on Na channels from rat cortical collecting tubule. American Journal of Physiology 253: F333-f339, 1987

Ussing, H. H., and K. Zerahn. Active transport of sodium as the source of electric current in the short-circuited isolated frog skin. Acta Physiologica Scandanavica 23: 110-127, 1951

This work was funded by the Wellcome Trust

Where applicable, the experiments described here conform with Physiological Society ethical requirements.

PC171

Systematic investigation of the role of the tyrosine residues in the transmembrane regions of the rabbit proton-coupled peptide transporter, PepT1

M. Pieri, C. Gan, C. Boyd and D. Meredith

Human Anatomy & Genetics, University of Oxford, Oxford, UK

The intestinal proton-coupled peptide transporter PepT1 mediates the uptake of di- and tri-peptides and peptidomimetic drugs in the intestine and kidney (reviewed by Meredith & Boyd, 2000). PepT1 has 12 transmembrane spanning regions, and it has previously been proposed that certain transmembrane(TM) tyrosines contribute to the transport function of human PepT1 (hPepT1: Y12 (TM1) and Y167 (TM5), Bolger *et al.* 1998; Y167, Yeung *et al.* 1998; Y56 and Y64 (both TM2), Chen *et al.* 2000). There are a further five TM tyrosines conserved between the mammalian PepT1 sequences: Y91 (TM3), Y287 (TM7), Y345 (TM8), Y587 (TM10) and Y648 (TM12). Here we report the results from a systematic investigation of their functional role in rabbit PepT1.

Individual tyrosine residues were site-directed mutagenised to phenylalanine in a rabbit FLAG epitope-tagged PepT1, the mutant PepT1 constructs expressed in *Xenopus laevis* oocytes, and the uptake of the neutral dipeptide [^{3}H]-D-Phe-L-Gln (0.4μM) measured (Panitsas *et al*, 2004). Data are mean ± SEM of 'n' oocyte preparations (5 oocytes per data point in each).

The Y91F mutant showed a significant decrease in [^{3}H]-D-Phe-L-Gln uptake (31.6 ± 5.7% of the wild-type, $p<0.05$, student's t-test) compared to the wild-type at pHout 5.5 (Figure 1A). In contrast, the Y287F, Y345F, Y587F and Y648F PepT1 mutants showed no apparent variation in uptake compared to the wild-type transporter. The Y12F and Y167F mutants gave similar results to those in the literature, with the exception of a measurable activity of Y167F (6.8 ± 0.9% of wild-type, compared to an abolished activity in HEK 293 cells, Yeung *et al.* 1998). Surface expression quantification by luminometry for Y12F, Y91F and Y167F suggested that the diminished uptake of D-Phe-L-Gln was not due to an effect on protein synthesis or trafficking (data not shown).

Computer modeling studies have predicted that Y91 had a role in proton interaction with hPepT1 (Bolger *et al.* 2000). To assess whether the tyrosine was important in the proton coupling of peptide transport, uptakes were performed at pHout 5.5, 7.4 and 8.4 (Figure 1B). For both Y91F and Y167F the pH dependence of uptake was similar to that of the wild-type PepT1.

In summary, we conclude that Y12, Y91 and Y167 play an important functional role in peptide transport by rabbit PepT1, as the mutant proteins showed reduced uptake rates. The exact mechanism by which this reduction in transport occurs still remains to be elucidated.

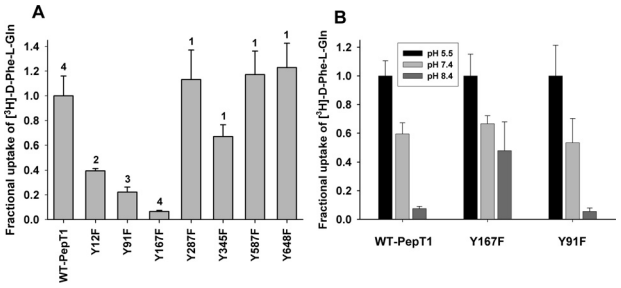

Figure 1A: Uptake of [3H]-D-Phe-L-Gln at pHout 5.5, normalized to wild-type (WT) PepT1 uptake (n value shown above each bar). Figure 1B: pH dependence of [3H]-D-Phe-L-Gln uptake, normalized to the uptake at pHout 5.5 for each construct (n=3 for Y167F, n=4 for WT-PepT1 and Y91F)

Meredith D & Boyd CAR (2000) *Cell Mol Life Sci* **57**, 754-778.

Bolger MB *et al.* (1998) *J Pharm Sci* **87**, 1286-1291

Yeung AK *et al.* (1998) *Biochem Biophys Res Commun* **250**, 103-107.

Chen XZ *et al.* (2000) *Biochem Biophys Res Commun* **272**, 726-730.

Panitsas *et al.* (2004) *J Physiol* **557P**, C56.

We thank the Wellcome Trust for generous funding.

Where applicable, the experiments described here conform with Physiological Society ethical requirements.

PC172

Mechanism of pH sensing in the two-pore domain potassium channel TASK2

A. Abohamed, M.J. Morton, A. Sivaprasadarao and M. Hunter

School of Biomedical Sciences, University of Leeds, Leeds, UK

TASK2 is a member of the two-pore domain potassium (K2P) channel family that plays a role in acid-base homeostasis; TASK2 knock-out animals have plasma electrolyte patterns typical of the human clinical condition of renal tubular acidosis (Warth *et al.*, 2004). It is expressed preferentially in epithelia, including the proximal tubules of the kidney. In common with the other TASK channels, TASK2 is sensitive to changes in extracellular pH, although the molecular mechanism of such pH-sensing is not understood (Morton *et al.*, 2003). We have examined the role of charged residues in the extracellular domains in pH-sensing in murine TASK2 using a mutational approach. Mutant channels were transiently expressed in CHO cells and studied by whole-cell and single channel patch clamp. Results are given as mean ± SEM with n, the number of observations. Statistical significance was assumed at $P<0.05$. Neutralisation of no single amino acid in isolation gave substantial loss of pH-sensitivity. However, the combined removal of five charged amino acids (E28, K32, K35, K42 & K47) in the large extracellular loop linking the first transmembrane and pore domains, the M1-P1 loop, resulted in a marked reduction in pH-sensitivity (WT = 84.6±0.02% inhibition at pH 5.8 v pH 8.8, n = 14; E28 = 21.1±0.05% inhibition at pH 5.8 v pH 8.8, n=8). This result was confirmed in single channel studies, where channels containing the five point mutations were stabilised in the open state. Wild-type channels contain two M1-P1 loops, but a concatemeric construct, comprised of one wild-type subunit and one containing the five mutations,

was fully pH sensitive, indicating that only one M1-P1 loop is required to yield a fully pH sensitive channel. This is the first demonstration of a regulatory role of this distinctive structure in K2P channels. Thus pH-sensing in TASK2 channels is conferred by the combined action of several charged residues in the large extracellular M1-P1 loop, and a single functional loop is sufficient for pH-sensing.

Morton, MJ *et al (2003). Pflugers Arch.* **445**, 577-583.

Warth R *et al.* (2004). *Proc.Natl.Acad.Sci.* **101**, 8215-8220.

This work was supported by The Wellcome Trust

Where applicable, the experiments described here conform with Physiological Society ethical requirements.

PC173

Multi-stage response of K^+ transport system to peroxynitrite action in human red blood cells

M.N. Starodubtseva[1] and J.C. Ellory[2]

[1]Chair of Medical and Biological Physics, Gomel State Medical University, Gomel, Belarus and [2]University Laboratory of Physiology, University of Oxford, Oxford, UK

Peroxynitrite ($ONOO^-$) is a powerful oxidant exhibiting a wide array of tissue damaging effects including lipid peroxidation, change in activity of enzymes and ion channel via protein oxidation and nitration (Szabo, 2003). Here we examined peroxynitrite-induced K^+ flux through the RBC membrane over a wide range of peroxynitrite concentrations (1-2000 μM) and its dependence on the time of peroxynitrite treatment (10-60 min). Peroxynitrite was synthesized from $NaNO_2$ and H_2O_2 and stabilized by alkali (Radi et al. 1991). Peroxynitrite was added as a bolus to the suspension of RBC (2-4% hematocrit), isolated from heparinised blood samples (from consenting volunteers with ethical permission), in buffer (NaCl or $NaNO_3$ 100 mM, Na_2HPO_4/Na_2HPO_4 50 mM, pH 7.4 or 6.8, 37ºC). K^+ influx was measured over 10 min at 37ºC using $^{86}Rb^+$ as a K^+ congener, in the presence of ouabain (100 μM), bumetanide (1μM), and clotrimazole (10 μM) to obviate influx via the Na^+-K^+pump, the Na^+-K^+-$2Cl^-$ cotransporter and the Gardos channel, respectively. Cl^--dependent K^+ influx was taken as a measure of K^+-Cl^- cotransporter (KCC) activity.

At peroxynitrite concentrations less than 300 μM, KCC is mainly activated with peak activity occurring at around 100 μM (KCC activity in control cells and cells after 100 μM peroxynitrite treatment was 0.56±1.46 mM (l cells)$^{-1}$ h^{-1} and 8.24±1.04 mM (l cells)$^{-1}$ h^{-1}, respectively, p=0.00016). This value correlates well with concentrations previously shown to produce maximum effects on tyrosine kinase activity in human RBC stimulated by peroxynitrite (Mallozzi et al. 1999). At higher concentrations, peroxynitrite treatment of RBC leads to an increase in Cl^--independent K^+-influx with the peak of delta[K^+]/delta[$ONOO^-$] at 220±48 μM (mean±S.E.M., n = 4), correlating with levels of methemoglobin formation and ATP depletion.

The effect on both Cl^--dependent and Cl^--independent K^+ fluxes induced by peroxynitirite was maximal following 30 min after peroxynitrite treatment. Neither $NaNO_2$, H_2O_2 or the products of peroxynitrite decomposition up to a concentration of 2 mM were able to induce an increase in Cl^--independent K^+ influx.

Analysis of the concentration and time dependences of Cl^--dependent and Cl^--independent K^+-influxes points to the presence of different sequential mechanisms underlying peroxynitrite actions on passive K^+ transport of human RBC.

Szabo C (2003). Toxicology Letters 140-141, 105-112.

Mallozzi C, Di Stasi AMM & Minetti M (1999). FEBS Lett 456, 201-206.

Radi R, Beckman JS, Bush KM & Freeman BA (1991). J Biol Chem 266, 4244-4250.

We thank The Physiological Society for financial support.

Where applicable, the experiments described here conform with Physiological Society ethical requirements.

PC174

A carboxy (C) terminal sequence in the rat $P2X_7$ receptor determines basolateral membrane targeting in MDCK cells

J. Owide[1], V.M. Collins[1], A. Surprenant[2], L. Jiang[1] and S.J. White[1]

[1]Biomedical Sciences, University of Leeds, Leeds, UK and [2]Biomedical Science, University of Sheffield, Sheffield, UK

Originally cloned from rat brain, the $P2X_7$ receptor is homologous to other P2X receptors but possesses a unique C-terminal tail that is required for the lytic actions of ATP that result in membrane disruption and both apoptotic and necrotic cell death (Surprenant *et al.* 1996). During kidney development, $P2X_7$ is expressed in differentiating collecting duct epithelia, and in the *cpk/cpk* mouse model of autosomal recessive polycystic kidney disease, collecting ducts express $P2X_7$ during fulminant cystogenesis (Hillman *et al.* 2002). Presently, it is not clear where in collecting duct cells $P2X_7$ is expressed, or by what mechanism(s) polarized membrane targeting occurs. Recent work suggests that the C-terminus is an important determinant of membrane trafficking of P2X receptors in neuronal cells (Chaumont *et al.* 2004). In this study we have tested whether the carboxy terminal domain is also important in polarized targeting of $P2X_7$ in renal epithelial cells.

MDCK monolayers grown on permeable filter inserts were transiently transfected with cDNA encoding wild type (WT) or mutant $P2X_7$ receptors in which the C-terminus (amino acids 362-595) was truncated either at residues 418 (G418) or at 570 (P570). All constructs were N terminally-tagged with the Glu-Glu epitope. At 72 h post transfection, the monolayers were fixed and the subcellular localization of each construct was determined by indirect immunofluorescence and confocal microscopy, using a commercially available antibody against the Glu-Glu epitope and an anti-rabbit Alexafluor^{488} secondary antibody. The localization of each construct was compared with that of endogenous domain-specific markers for (a) the basolateral membrane (β-catenin), detected by indirect immunofluorescence using a commercially available primary antibody and a Cy5-conjugated secondary antibody and (b) the apical membrane detected with rhodamine-conjugated peanut agglutinin (PNA). Transfections were replicated between 3 and 5 times for each construct.

All appropriate antibody controls were negative. WT $P2X_7$ colocalized with β-catenin in the basolateral membrane and no fluorescence could be detected in the apical membrane. In contrast, both the G418 and P570 $P2X_7$ constructs colocalized both with

β-catenin in the basolateral membrane, but also with PNA in the apical membrane.

From these experiments, we conclude that rat $P2X_7$ is targeted to the basolateral membrane of renal tubular cells and that the C-terminus is important in determining appropriate membrane targeting. From the targeting pattern of the G418 and P570 mutants we propose that amino acids 570 - 595 may contain a motif (yet to be identified) that is necessary for discrete basolateral sorting of $P2X_7$.

Surprenant A *et al.* (1996). *Science* **272**(5262), 735-8.

Hillman KA *et al.* (2002). *Exp Nephrol* **10**(1), 34-42.

Chaumont S *et al.* (2004). *J Biol Chem* **279**(28), 29628-38.

This work was supported by the University of Leeds. V.M.C. was a recipient of a "White Rose" Scholarship.

Where applicable, the experiments described here conform with Physiological Society ethical requirements.

PC175

Potassium channel mRNA expression in human colon cancer

J.E. Linley[1], G.I. Sandle[2] and M. Hunter[1]

[1]BMS, University of Leeds, Leeds, UK and [2]Molecular Medicine Unit, St James's University Hospital, Leeds, UK

Colorectal cancers are a major cause of death; many start as adenomas, growing and becoming dysplastic, with an increasing risk of malignant change. Dysplastic transformation is associated with depolarisation of the crypt epithelia cells, possibly indicating a change in K channel regulation or expression. Three K channel species have previously been identified in human colonic crypt cells by functional and RT-PCR studies: KCNQ1/KCNE3, KCNN4 and KCNMA1 (Sandle *et al.* 1994; Morton *et al.* 2001). Using real-time quantitative PCR (Lightcycler, Roche), the mRNA expression of K channels was measured in human colonic cancer and macroscopically normal adjacent tissue. Tissue was obtained, with consent and local ethical committee approval, from patients undergoing tumour resection. Tissues were embedded in optimum cutting temperature (OCT) medium, snap-frozen and sliced on a cryostat. RNA was isolated using the TRIzol method with 1μg total RNA added to the reverse transcription reaction. K channel mRNA expression was determined using the delta CP method (Pfaffl, 2001) and normalised to β-actin and 28-S RNA levels.

Expression of the basolateral small conductance K channel encoded by KCNQ1 and its associated β subunit KCNE3, were both significantly elevated in the cancer by 2.6 ± 0.5 and 2.5 ± 0.5-fold, respectively (mean ± SEM), ($p<0.05$, $n = 8$). Similarly the basolateral intermediate conductance K channel (KCNN4) was increased by 3.0 ± 1.3-fold in the cancer tissue ($p<0.05$, $n = 8$). However, mRNA for the apical large conductance K channel (KCNMA1) was unchanged (1.0 ± 0.3-fold change, $p>0.05$, $n = 8$). Statistics were performed on log transformed data using a 1-tailed t test.

This study shows that the mRNA expression of KCNN4 and KCNQ1/KCNE3 is increased in colon cancer, whereas KCNMA1 appears unchanged. If the changes in K channel expression observed in colon cancer are mirrored in adenomatous polyps, then these channels may provide a biomarker for malignant potential.

Sandle GI *et al.* (1994). *Lancet* **343**, 23-25.

Morton MJ *et al.* (2001). *J Physiol* **535P**, S006.

Pfaffl MW (2001). *Nucleic Acids Res* **29**, 2002-2007.

This work was funded by the Yorkshire Cancer Research Trust.

Where applicable, the experiments described here conform with Physiological Society ethical requirements.